Technical report, IDE0953, November 2009

Design and Implementation of an Ion Beam Profiling System

Master's Thesis in Electrical Engineering

Joan Stude

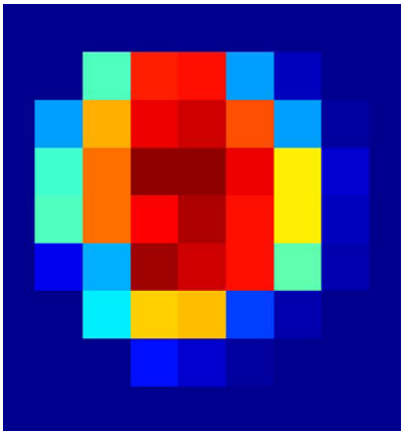

School of Electrical Engineering

Solar System Physics and Space Technology

ION BEAM PROFILING SYSTEM

Master's thesis in Electrical Engineering

Institutet för rymdfysik

School of Information Science, Computer and Electrical Engineering
Halmstad University
Box 823, S-301 18 Halmstad, Sweden

Kiruna, Sweden, November 2009

I would like to thank my parents for supporting my studies in Sweden.

I also would like to thank my supervisor, Martin Wieser, for the good advice he gave and the whole staff at IRF for supporting the work at any time.

Description of cover picture: a typical ion-beam profile, taken with the system described in this thesis

Abstract

The work describes the development of a reliable device for profiling an ion beam in the intensity cross section. A sensor head consisting of a Faraday cup in combination with a Channel Electron Multiplier was designed and built together with electronics including power supply and front end electronics. The design was chosen considering financial and long term life aspects. Testing, first calibration and error analysis were done using the ion beam facilities where the unit is supposed to be installed permanently. The profiling system performed as designed and the profile of the ion beam could be measured reliably with an accuracy down to the femto ampere range.

Contents

1 Introduction **7**
- 1.1 Announcement of Thesis . . . 7
- 1.2 Introduction . . . 7
- 1.3 Beamline . . . 9

2 Sensor **10**
- 2.1 The Scanner Unit . . . 10
- 2.2 Sensor Head . . . 11
  - 2.2.1 Channel Electron Multiplier - KBL series . . . 13
  - 2.2.2 Faraday Cup . . . 16

3 Electronics **18**
- 3.1 CEM electronics . . . 18
  - 3.1.1 CEM Pulse Transmission and Detection . . . 19
  - 3.1.2 CEM High Voltage Power Supply . . . 20
- 3.2 Faraday Cup electronics . . . 21
  - 3.2.1 AD-Converter . . . 25
  - 3.2.2 Suppressor electrode . . . 26
- 3.3 Controller & Interfaces . . . 26
  - 3.3.1 Motor controller . . . 26
  - 3.3.2 Power supply . . . 27
  - 3.3.3 Sensors . . . 27
  - 3.3.4 Server . . . 28
- 3.4 Power considerations . . . 28
- 3.5 Schematic & Layout . . . 29

4 Tests and Results **30**
- 4.1 Setup . . . 32
  - 4.1.1 Beam . . . 32
  - 4.1.2 Mechanical . . . 32
  - 4.1.3 Electrical . . . 33
  - 4.1.4 Measurements . . . 33
- 4.2 Results . . . 35
- 4.3 Discussion . . . 41
- 4.4 Outlook . . . 43

5 References **44**

Lists of Figures **45**

List of Tables **46**

A Abbreviations **46**

B Schematic Power Board **47**

C Schematic Front-End Electronics **48**

1 Introduction

1.1 Announcement of Thesis

"Design and implementation of an ion beam profile scanner

The purpose of this hardware project is to design, implement and calibrate a scanning ion beam monitor for IRF's ion calibration system. The knowledge of the ion beam intensity and profile is the starting point for all instrument calibrations. The new design should be able to ultimately replace the present system in terms of flexibility and usability. The new system will need to be integrated with currently used monitoring systems and the corresponding generic data acquisition system."

Contact person: Dr. Martin Wieser (martin.wieser irf.se, +46 980 79198)

1.2 Introduction

The Solar System Physics and Space Technology (SSPT) research program at the Swedish Institute of Space Physics (IRF) in Kiruna works mainly on three topics: instrument development, data analysis and computer modeling on the interaction of the solar wind with the space environment of planets, moons, asteroids, comets and even exoplanets. The instruments such as ion mass spectrometers, electron spectrometers or energetic particle detectors are completely designed, built and calibrated in their own facilities.

Current examples are:

- ASPERA-3/4, an analyzer of ions and energetic neutral atoms, which is part of the scientific payload on Mars & Venus Express
- MIPA, a miniature ion precipitation analyzer, part of the SERENA instrument which will be on board BepiColombo heading for Mercury.
- SARA, which travels on board Chandrayaan-1 to analyze neutral atoms reflected from the surface of the Moon.

To test and calibrate such instruments an artificial signal source is needed. The solar wind is a plasma coming from the sun. The particles (ions, electrons and atoms) approximately represent the composition of the sun and are mainly hydrogen or helium ions but also heavier particles like iron for example [6]. A laboratory with a vacuum chamber exists for this purpose, the calibration lab. It is equipped with an electron source and an ion source (figure 1a). The ion beam enters from the right side and the electron beam enters from above (not shown). In the center there is a table for the devices

under test which allows position and orientation adjustment in four degrees of freedom.

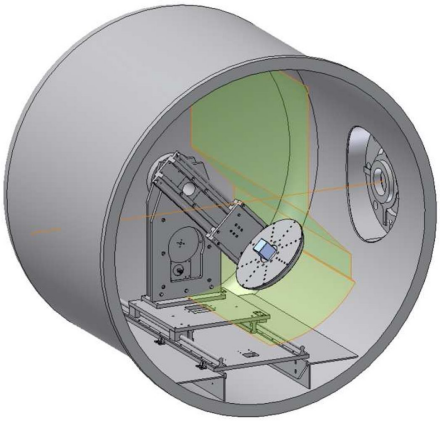

(a) The chamber in present condition (2009)

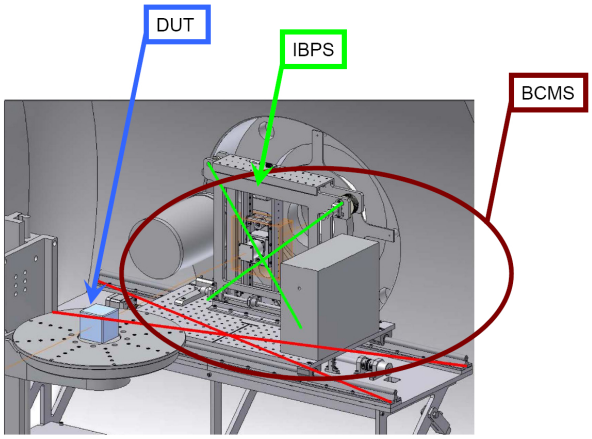

(b) desired enhancement

Figure 1: Vacuum chamber for calibration

Testing and calibrating takes a lot of time and effort. Therefore the idea is to improve this procedure in terms of time and usage with additionally more accuracy with an automatic ion beam profiling system. The planned new parts to support the ion beam profiling system are shown in figure 1b. The red cross shows a linear table to place different auxiliary instruments into the beam without the need to open the chamber. The green cross marks the 2-dimensional profile scanner. The table and the scanner form together the Ion Beam Characterization and Manipulation System (BCMS).

One important calibration issue is the geometric factor of an instrument.

It is necessary to know how sensitivly it measures incoming ion flux, so the beam should have well-known properties. Among these properties such as energy, charge or mass of the incident ions, one is the intensity distribution over the beam cross-section, the profile. The problem is that the beam is not constant over time and is strongly dependent on ion-source settings. So a scanner was designed to get within reasonable time steps an actual beam profile. The objective of this thesis is to design a sensor head with the corresponding electronics taking into account the needs and experience of the researchers and the feasible solutions from a mechanical point of view. It should use existing technology and knowledge to produce a helpful and reliable measuring tool.

1.3 Beamline

The ion beam system in the calibration lab is the PSX-2751 50keV Ion Source from Peabody Scientific which uses a duoplasmatron source for creation of the necessary ions. A discharge from a Barium-oxide coated filament to an anode generates a dense ionizing electron flux. Via a gas inlet, Argon, Hydrogen and Air are leaked into the discharge volume, creating a lot of different ions simultaneously by collisions: e.g. $H^+; N^+; Ar^+; C^+$ etc. Beside the ions also small amounts of energetic neutral atoms and even X-rays are created. The ions are then extracted by a high voltage of up to 50kV which draws the ions through a small aperture.

After this the beam passes an Einzel lens, a Wien-Filter, an electrostatic analyzer and two more Einzel lenses. The first lens focuses the beam whereas the last lens broadens it. The Wien-Filter ($E \times B$) applies an electrical and magnetic force to the ions in such a way that only particles with a certain energy and mass per charge (or velocity) can pass. The Electrostatic Analyzer (ESA) provides a 90° angle to prevent energetic neutral atoms and X-rays from entering into the chamber. The chamber is capable of maintaining a pressure down to $10^{-7} mbar$.

To monitor and measure the total ion beam current a grid and a big Faraday cup are currently installed. The grid covers the whole beam entrance and gives an approximate beam current value. The advantage with the grid is a continuous monitoring of the total ion beam current while passing around 90% of the beam. The big Faraday cup is more exact but blocks the beam completely.

The final parallel beam has intensities up to $100nA$ and diameters up to $100mm$ with selected energy and mass. The beam is adjustable in intensity and profile but also time dependent (Peabody describes this as a stability less than 2% over 10 minutes). From that we get a constraint in which

one complete profile has to be ready which is assumed with 5 minutes at maximum. This ensures that a later measurement is always correlated to a profile.

2 Sensor

2.1 The Scanner Unit

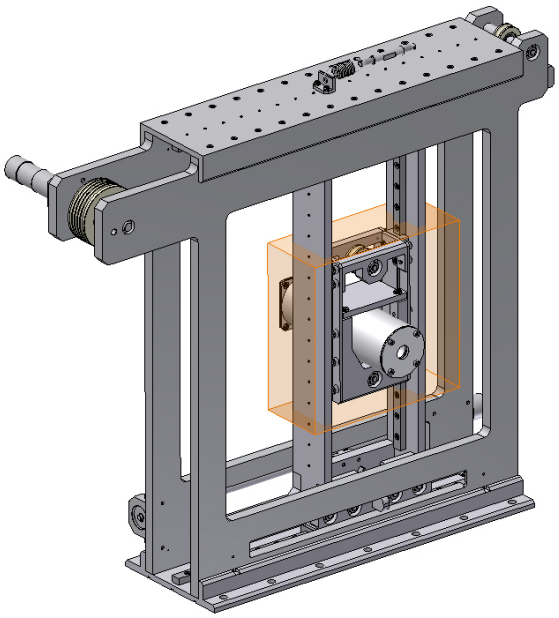

Figure 2: Beam scanner with Sensor head

Figure 2 shows the entire beam scanner including sensor head. The red area marks the scanning field of $120 \times 120mm$.

The idea is to have an actual profile for every series of measurement done with a device under test. So when the scanner is in position it should do a profile as fast as possible but at least within 5 minutes (beam stability). The advantage of that rather complex mechanical structure is that the motors are mounted in a fixed position in the structure. Motors tend to disturb a charged particle beam with their magnetic fields. If the motor was in the moving parts the profile would become dependent on the motor position. Additionally the sensor needs enough freedom to move completely out of the beam. The Scanner therefore has a parking position to let the beam pass without disturbance.

For all the mechanical aspects see the work by Jérôme Lescoup[5]. The motors to move the scanner and the table will be stepping motors with attached quadrature encoders controlled by a dedicated unit which should be independent from all other systems. The solution for that was found in the TMCM-351 from TRINAMIC motion control. It offers 3-axis control on a single board (Eurocard), drivers, encoder interface and several communication pipelines to interface with.

2.2 Sensor Head

The flux of particles with mass and charge in an ion beam can e.g. be detected by conversion of kinetic energy to form secondary particles {a} or by deposition of charge {b}. Common detectors using these principles are:

- the Channel Electron Multiplier (CEM){a}
- the Micro Channel Plate (MCP){a}
- the Scintillator (Scint.){a}
- the Faraday Cup (FC){b}

A classical combination is the Micro Channel Plate with a scintillator. This offers high resolution (μm^2) but is limited in measuring equivalent current due to saturation effects in the small channels. Another disadvantage is the energy dependent count rate because of the scintillator. Using the full ability of spatial resolution will also cause high costs. Even so in case that resolution would be the main constraint a MCP-based solution is feasible. Because in the present system a resolution of $10mm^2$ is enough and the dynamic range of the desired measurement is high, a combination with a Channel Electron Multiplier and a Faraday cup was chosen. A Faraday cup can measure almost any current down to its noise level. The CEM suffers in principle from the same saturation effect as the MCP but in combination with the FC a very high dynamic range results, from single ions up to rather high currents. The drawback here is that this sensor has no inherent spatial resolution. To get a profile of pixels the sensor has to be moved to scan the beam. For this reason a mechanical scanner was constructed to carry a sensor head built upon a Channel Electron Multiplier and a Faraday cup. Another point was the availability of CEM's at IRF.

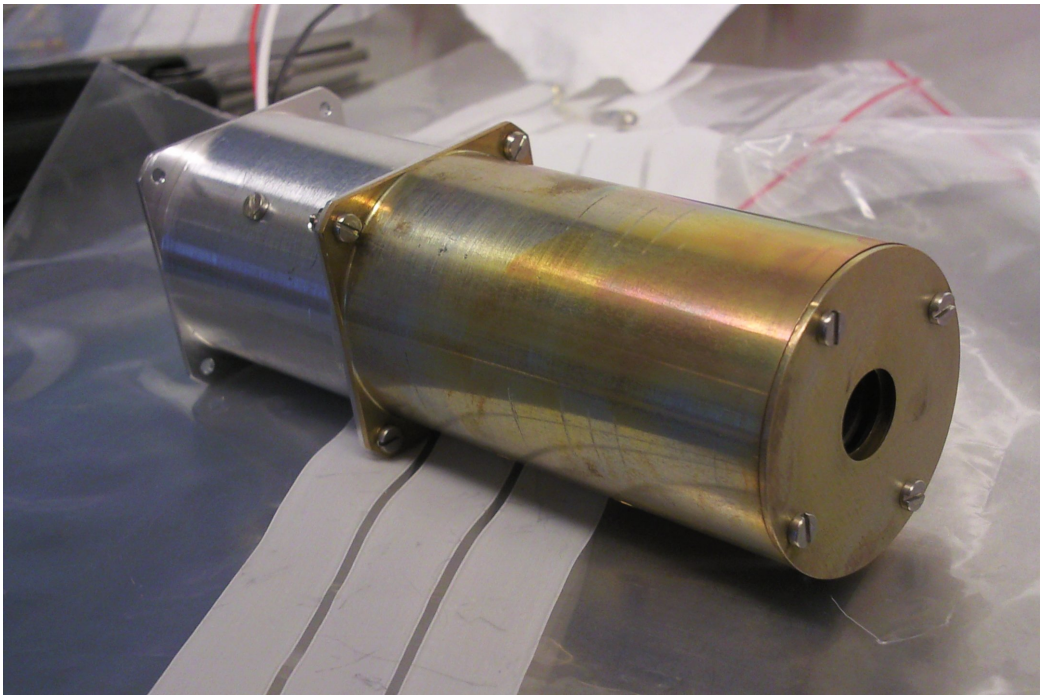

Figure 3: Sensor head; the front housing surface for the Faraday cup is already passivated with iridite (yellowish)

2.2.1 Channel Electron Multiplier - KBL series

A CEM uses the kinetic effect to create an electron shower which can be measured as a current pulse. A channel with a high resistive coating forms a continuous dynode. A dynode can simultaneously act as a cathode and anode (dyo = "two") which means it can absorb and emit electrons at the same time. The resistive coating ensures a gradual increase of voltage to accelerate the electrons which is shown in figure 4.

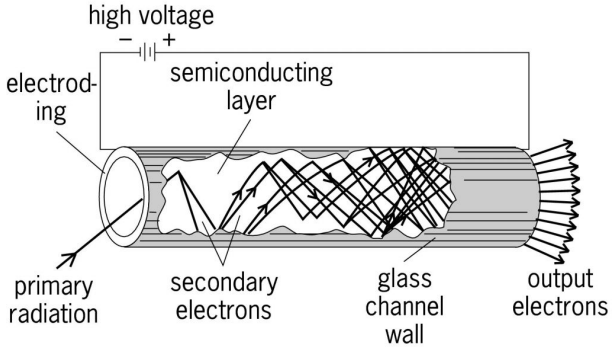

Figure 4: Cutaway view of a straight, single-channel electron multiplier, showing the cascade of secondary electrons resulting from the initial, primary radiation event, which produces an output charge pulse. (After J. L. Wiza, Microchannel plate detectors, Nucl. Instrum. Meth., 162:587–601, 1979)

This avalanche of electrons needs just a few steps to create up to 10^8 comrade electrons from one single electron. At the end of the channel an anode collects the electron cloud and hence a readable current pulse is achieved. The minimum time between two pulses (count rate) depends on the resistive coating (wall resistance). Each pulse represents one ion and when counted within a certain time an equivalent current can be calculated with:

$$I_{CEM} = \frac{n}{t} \cdot e \tag{1}$$

IRF uses CEM's from the company "Dr. Sjuts Optotechnik GmbH", in this case the "KBL 408". It has a length of $26mm$. In picture 5 one can see the well-curved channel of the CEM. To the left the blueish triangle represents the entrance and on the right side one can see the anode.
"The curvature of the channel is necessary to prevent ion feedback caused by the high electron density at the end of the channel. In a straight channel ions would pick up too much kinetic energy and generate additional secondary electrons leading to an unstable operation of the CEM."(taken from [4])

The basic structure of the CEM is made out of ceramics which is coated with glass and additional layers from both sides. Some technical parameters

Figure 5: KBL408

are shown in table 1.

parameter	value
Typical gain at 2.3 kV applied voltage :	$1 \cdot 10^8$
Typical wall resistance	$200 M\Omega$
Pulse height distribution at 2.6 kV and 3.000 cps	$< 50\%$
Dark count rate above a threshold of - 5 mV	$< 0.02 cps$
Maximum count rate cps	5 Mio
Typical pulse width (FWHM) at 2.3 kV	$8 ns$
Operating voltage	max. $3.5 kV$
Temperature (operating and storage)	°C max. 70

Table 1: Data from CEM KBL series

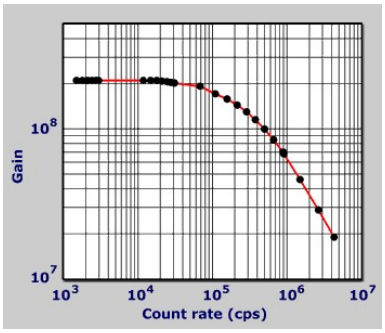

Figure 6: Gain vs. counts from `http://sjuts.com/CEMModels_Standard.html`

Figure 6 shows the gain of a CEM against the count rate. The point where the gain starts to decrease is at around a count rate of $5 \cdot 10^5 cps$. Ideally the FC should give values for the beam intensity from this point on to extend the measurement range. This upper value for the equivalent beam current in the CEM is:

$$I_{CEMmax} = 5 \cdot 10^5 cps \cdot e = 80 fA. \tag{2}$$

The next part of the sensor head, the Faraday cup, should provide a smooth overlap in terms of equivalent beam current to the CEM. At this point both sensors should give clear results and thus provide the possibility to switch between them.

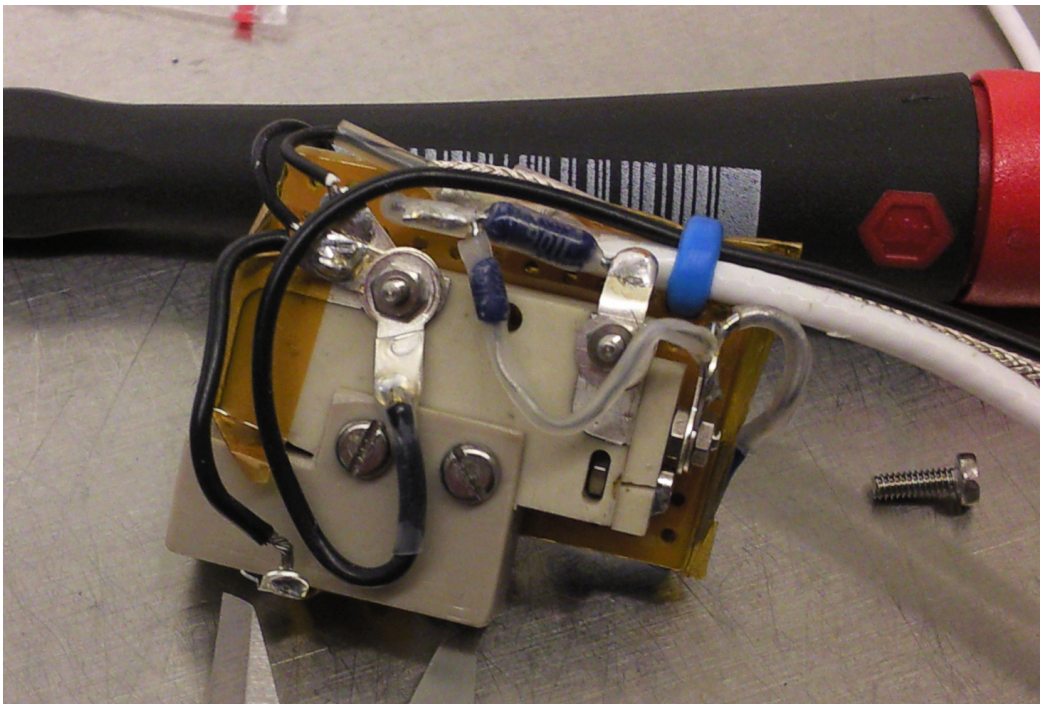

Figure 7: Fully assambled CEM ready to be mount in the sensor head. The entrance to the left still covered, the 2 resistors in the middle and the anode to the right.

2.2.2 Faraday Cup

A Faraday cup is basically a simple metal can. It is placed in a beam of charged particles (vacuum) to absorb them. When they are caught they charge the metalcup. An amperemeter can now measure the current and thus the amount of particles. The direction of the current depends on the sign of the charge from the ions which building up the beam current. The device is named after Michael Faraday who first predicted ions around 1830.

The Faraday cup is cylinder- shaped and is made from Aluminum. The starting point for the construction is the needed spatial resolution of $10mm$. So the FC will have a round opening of $10mm$ in diameter. It needs to be at least 2 times deeper than it is wide to hinder particles from escaping the cup. Inside the cup the surface is sandblasted to avoid specular reflection and to improve absorption. Usually there is also a skewed surface inside the cup but in this sensor it was not installed because of the connected CEM behind. Instead the depth is relatively high at $40mm$. The current to be measured is a flux of electrons into the FC to balance the incoming positive charges. But these incoming ions create secondary electrons which are very mobile and need to be confined in the cup. Every lost electron will look in the measured current like an additional ion. A common way to prevent electrons escaping is a suppressor electrode (SE). That is why the FC is additionally equipped with an aperture plate at the entrance. A negative potential at this electrode will form a potential wall, preventing electrons from escaping.

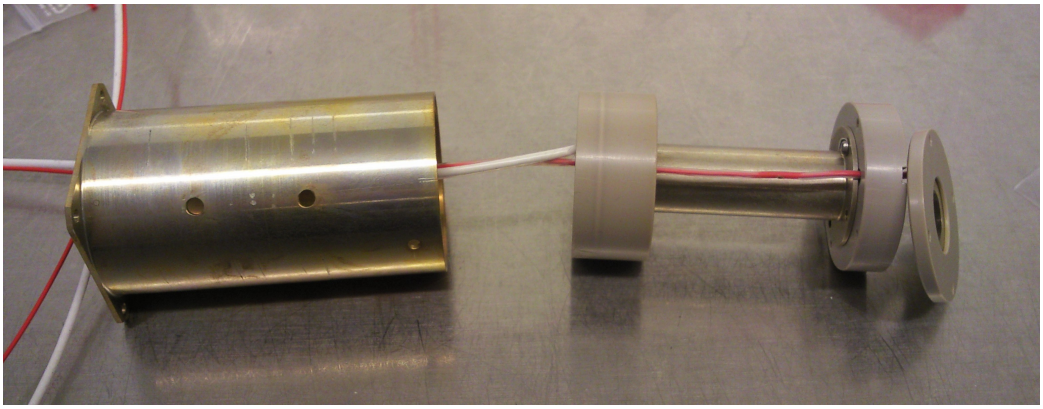

Figure 8: Housing and Faraday cup; the cup is bed in isolation material, to the right is the suppressor electrode; the red wire is connected to the suppressor electrode and the white on is connected to the bottom of the Faraday cup

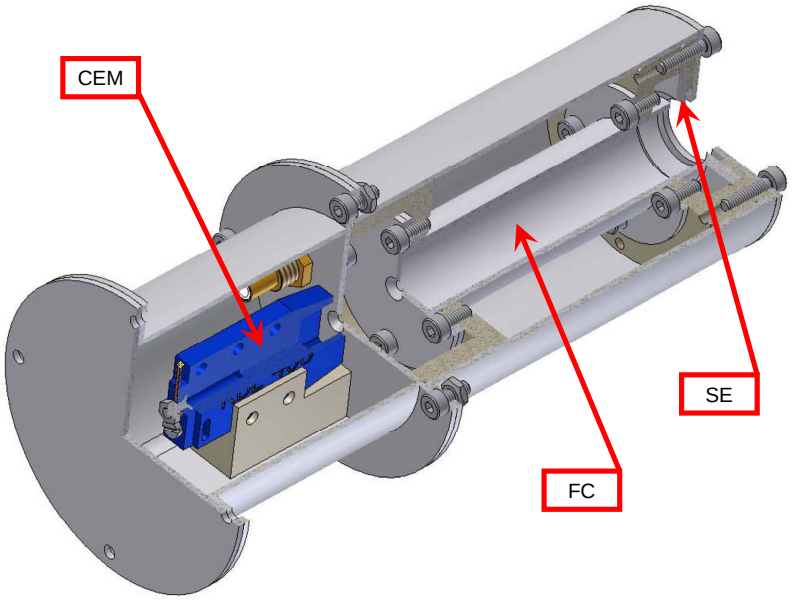

Figure 9: The Sensor head

The CEM is placed behind the FC in order to be aligned with the beam. The bottom of the FC is also the aperture for the CEM. With this a ratio of beam current between FC and CEM is set. If the hole is too big, the FC is probably still in its noise level when the CEM is already at maximum count rate. If the hole is too small, the CEM will have a too low count rate. It was decided to go for a diameter of $2mm$ which results in a FC-current at a maximum CEM count rate of:

$$I_{FC} = \frac{A_{FC} - A_{CEM}}{A_{CEM}} \cdot I_{CEMmax} = 24 \cdot 80fA = 1920fA \approx 2pA \qquad (3)$$

I_{FC} is the current in the Faraday cup and A is the appropriate detection area.
So when the CEM is measuring $80fA$ equivalent current the Faraday cup draws a current of $2pA$ which marks the overlapping point and gives a minimum value for the current measurement. The FC is well isolated (PEEK and free space) from the outer enclosing to avoid collection of unwanted charges. The enclosure is connected to ground for shielding.

3 Electronics

3.1 CEM electronics

The electronics for the CEM consists of three parts:

- adjustable power supply: $\approx 3kV$
- transmission line: $\approx 125MHz$
- discriminator and pulse former: $\approx 1MHz$

The CEM has three connectors: the entrance of the channel, the output of the channel and the anode for collecting the electrons. The entrance should be at zero volts to minimize influences on incident particles. That implies that the output has to be at a high positive potential to accelerate the secondary electrons. The anode must be at an even higher potential to further accelerate the electrons out of the channel. This ensures maximum gain and narrow pulse height distribution. Sjuts recommends around $100V$ between anode and channel outlet. To achieve this a resistor in series with the channel (wall resistance) forms a simple voltage divider. A value of $\frac{1}{25}$ of the wall resistance is recommended by Sjuts.

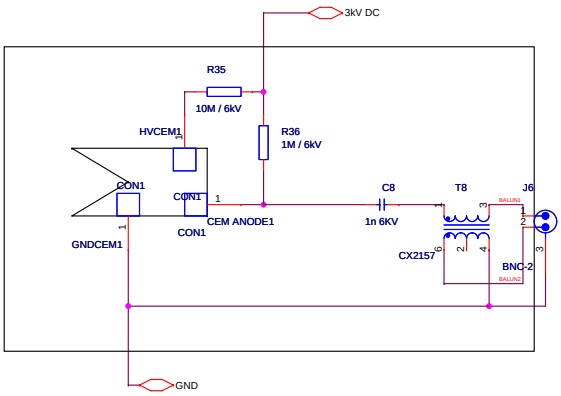

Figure 10: Connections of the CEM

As seen in figure 10 a $10M\Omega$ resistor (R35) is used for the voltage divider. The anode is floating via a $1M\Omega$ resistor (R36) on the full high voltage. The capacitor becomes necessary in this arrangement to decouple the high voltage from the low voltage detecting circuit. Recommended values are between $0.15nF$ and $1nF$. The higher value gives lower losses, so $1nF$ is used.

3.1.1 CEM Pulse Transmission and Detection

The transmission of the pulses is a concern because the discriminator is placed outside the vacuum chamber with a transmission length of approximately $2m$ in generally noisy environment. The expected pulses have a FWHM of $8ns$ (see table 1) which gives a pulse length (l_p) of:

$$l_p = c_0 \cdot \frac{1}{\mu_r \epsilon_r} \cdot FWHM \approx 1.7m \tag{4}$$

The velocity factor $\frac{1}{\mu_r \epsilon_r}$ is due to the slower propagation of electro-magnetic waves in different environments than vacuum. The constants are depending on the isolation material which is PE ($\mu_r = 1$; $\epsilon_r \approx 2.3$) The calculated pulse length shows that careful design is needed because the transmission line exceeds the pulse length and reflections may become a problem. Connectors, cable, feed-troughs and other parts have to be impedance matched to avoid reflections.

For a noisy environment it is beneficial to have a differential (symmetrical or balanced) signal that cancels out common mode noise and and enables the use of twisted pair cable to cancel out induced noise. The only way to achieve a passive conversion from a single ended or unbalanced line to a balanced one is to use a BALUN or in this case an UNBAL. BALUN stands for BALanced UNbalanced. BALUN's are transformers which are very common in audio and video transmission. There are 2 types of baluns, voltage and current (choke) baluns. The voltage balun provides galvanic separation and a first order high-pass whereas the current balun provides a first order low-pass. The names come from the fact that in a current balun the currents in each coil have equal sign, whereas in the voltage balun the voltages are equal. Beside this conversion both are also used for impedance matching. From a former development at IRF for its MIPA (Miniature Ion Precipitation analyzer) instrument on the BepiColombo mission such a transmission for CEM pulses was investigated and tested. The result was a combination of both types as depicted in figure 11.

Directly after the decoupling capacitor a current balun is used for generating the differential signal. The output of the transmission line (twisted pair) uses the voltage balun to recreate the unbalanced signal needed for the A101. The baluns are chosen to have small losses in the desired frequency band, in this case around $1dB$ of insertion loss from the data sheet.

The short pulses from the transmission line have to be shaped to interface to a counting input of a microprocessor. For this a ready and widely used circuit is available. The discriminator A101 from AMPTEK is specially designed to interface to multiplier tubes. It integrates the incoming pulse to

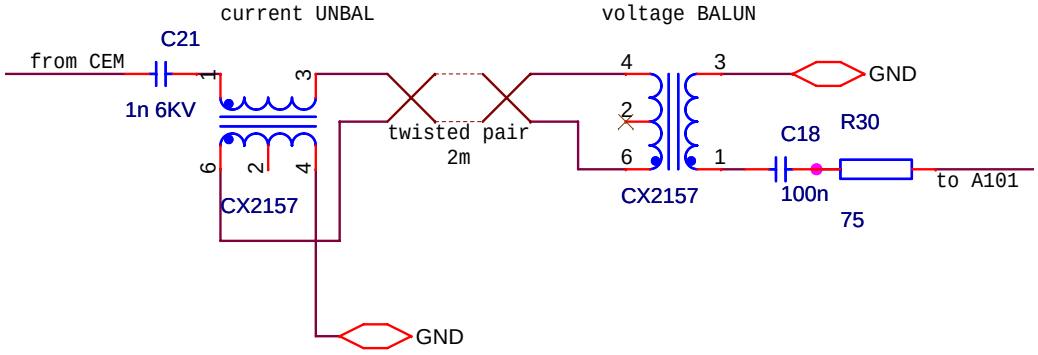

Figure 11: Transmission of CEM pulse via BALUN's

get its charge and outputs a TTL pulse. Such devices are also called charge sensitive preamplifiers. The A101 is sensitive down to $0.16pC$. If another input pulse reaches the A101 before the output pulse is finished the input pulse is not registered. It is capable of a maximum count rate of $4MHz$.

3.1.2 CEM High Voltage Power Supply

The CEM needs an adjustable Voltage V_{CEM} up to $3.5kV$. The current needed is at least $17\mu A$.

$$I_{CEM} = \frac{V_{CEM}}{R_{CEM}} = \frac{3500V}{200M\Omega} \approx 18\mu A \tag{5}$$

R_{CEM} is the wall resistance from the CEM. A high voltage power supply (HV-PS) design from the PRIMA (Prisma ion mass analyzer) instrument for the Swedish mission PRISMA was adapted. The HV-PS was designed for exactly the kind of CEM's as used in the present project. It offers the voltage range needed, enough power as well as adjustment and monitoring. It is based on a switching transformer circuit with a voltage multiplier attached.

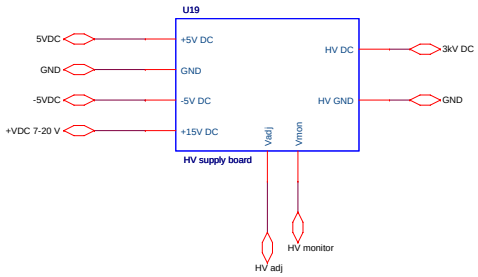

Figure 12: Connections of HV Board

To operate the supply, $\pm 5V$ DC and $15V$ DC as power inputs are required. The adjustment of V_{CEM} is done with a reference voltage from 0 - 4 volt at the Vadj Pin in figure 12. The monitoring output is derived from the voltage output with a resistor divider and then normalized to 0 - 3 volt. This port is read by the micro controller to record the output value. The reference voltage and therefore the output is controlled via a variable resistor divider. In case it is needed it could also later be controlled via a processor.

3.2 Faraday Cup electronics

The electronics for the Faraday cup consist of a current measurement system with digital conversion. There are basically two ways, to detect low currents, the shunt method or the transimpedance method. For the shunt method the current is simply fed through a resistor and thus converted to a voltage which is then amplified and measured. A transimpedance amplifier converts the current into a voltage via an operational amplifier. The big advantage with an ion beam is that it can be seen as an almost ideal current source, which makes it possible to work with both methods. The transimpedance amplifier is more common because of the faster response and because no current leaks out of the measurement line due to the low input resistance. The faster response arises from the fact that the input capacitance is not charged as in the shunt method. A typical coaxial cable has a capacity of $100pF$ per meter which easily causes a measurement time larger than $1s$. The transimpedance method is therefore advantageous. To pass the small current out of the chamber, a triaxial cable should be used for best performance. Because the equipment for this, such as connectors and feed-throughs is rather expensive and bulky, a coaxial solution was used. The

guard shield in such a cable is mainly to hold back leakage current and it is assumed that it can be tolerated. To measure a current of $2pA$ as stated in 2.2.2 an accuracy of current is set to $200fA$. Designing an amplifier circuit for this low current can be very tricky. A conventional bipolar OpAmp would have some μA as input bias current which would be devastating. From that point of view the input bias current is the most important parameter for choosing an OpAmp. An investigation showed that operational amplifiers are on the market with down to $20fA$ of initial input bias-current. A good solution was found from National Semiconductor with the LMP7721 ([3]). Including the optional evaluation board it was offered for a price of $US15. Table 2 shows some of the maximum parameters for $25°C$.

Parameter	Value
Input Offset Voltage	$\pm 150\mu V$
Input Bias Current	$\pm 20fA$
Gain Bandwidth Product	15MHz
Common Mode Rejection Ratio	$100dB$

Table 2: LMP7721

Also OpAmps such as the LTC6078 have less offset voltage but the parameter is less important than the input bias. Furthermore the LMP7721 has an improved pin-out for sensitive measurements. The evaluation board is specially designed featuring a complete guard ring and guard driver to enable full performance. A guard is a voltage that is kept at the same potential as the signal line and thus reducing leakage to zero. Such a guard ring surrounds the whole input-system.

For the current-to-voltage converter (as the transimpedance amplifier is also called) the feedback resistor has to be determined. This resistor determines the conversion as shown in equation 6:

$$I_{FC} = -\frac{V_{out}}{R_F} \tag{6}$$

It is assumed that a voltage step of $1mV$ is a clear signal. Together with the current accuracy of $200fA$ a resistor of $5 \cdot 10^9\Omega$ is needed. To get a more easily readable value and add some margin a $10G\Omega$ resistor was chosen for the feedback path. This gives a current-to-voltage ratio of $10^{10}V/A$. The resistor could be changed with no effort if the overlap point to the CEM measurement range needs to be adjusted. Attention should be paid that only resistors with an accuracy of $\leq 1\%$ are used. The maximum of this resistor is assumed to be 1% of the input resistance of the OpAmp or other involved parts as the

later mentioned range switch. Surface resistance, leakage and noise pick up will also determine if a value is feasible or not. The input resistance from the LMP7721 is not mentioned in the data sheet. From a compareble OpAmp (LMC6462) a value was found with $> 10T\Omega$. So to keep the error low, the resistor's upper limit value would be 1% of $10^{13}\Omega$ which is $100G\Omega$.

With this resistor the maximum detectable current is also set according to the maximum output voltage of the amplifier. The $10G\Omega$ resistor with the supply voltage ($2.5V$) of the opamp limits the maximum measurable current to $250pA$. Depending on the desired maximum beam current the range can be extended. A solution for this is to switch a parallel resistor into the circuit. Figure 13 shows the circuit from the evaluation board with the relay for the range switch. The second OpAmp LMP7715 is operating as a guard driver.

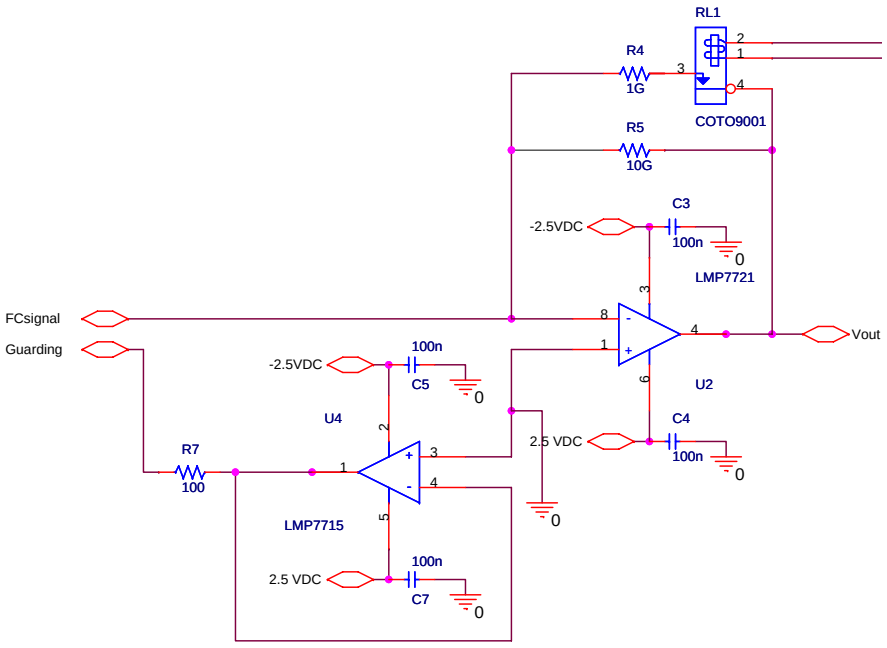

Figure 13: Transimpedance Amplifier

The range-switch will be a critical point because of its implementation in the feedback path. Leakage and parasitic resistance/capacitance have to be considered. The open contact should have a low capacitance because it affects the measurement time and it needs a high resistance to keep the accuracy. The open contact resistance should be around 100 times more than the initial feedback resistor whereas the capacitance should not be more

than $10pF$. With closed contact the applied voltage could cause a significant current into the feedback path. So the contact has to be placed at the output of the OpAmp where it has no impact at the measurement. Most relays tend to have several giga ohms resistance between contacts which would be too low. Reed relays are improved with regard to this point. With COTO[1] a company was found to provide a minimum resistance of $10^{12}\Omega$ between contacts and capacitance as low as $0.7pF$. In the circuit (fig. 14) the relay will be controlled via a pnp-transistor on the high-side to keep the relay coil un-powered in switched-off state. Otherwise probably even $5VDC$ would cause a leakage current of $5pA$ over the relay contacts. The second npn-transistor interfaces to a 3.3V controller port. Furthermore a zener diode and a normal diode are placed close to the relay to ensure maximum switching speed and safety for the transistors by suppressing the coil voltage transient as recommended in the data sheet. The transistors should withstand this rather high zener voltage.

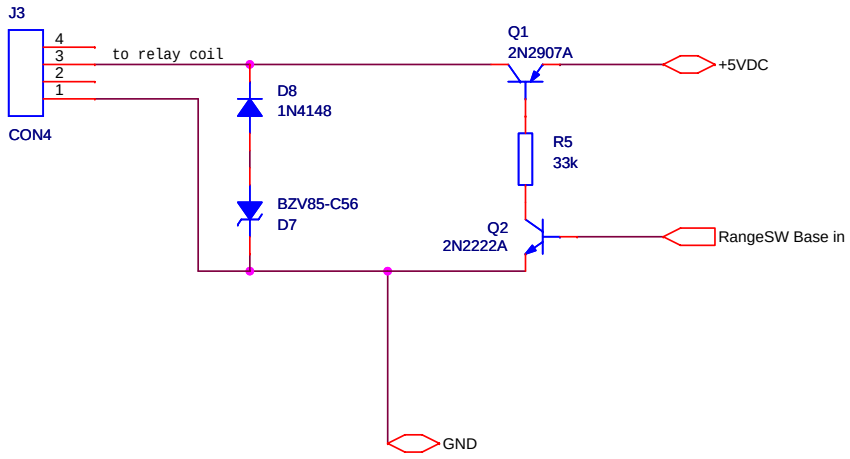

Figure 14: Relay control

[1] `http://www.cotorelay.com/html/reed_relays.html`

3.2.1 AD-Converter

To digitize the output values of the transimpedance amplifier an analog/digital converter (ADC) is needed. The output of the LMP7721 will be in the range of $+2.5V$ to $-2.5V$ depending on the charge of ions in the beam. Thus the input of the ADC should be a bipolar one. The conversion speed needed is at minimum 10Hz, but with every additional converted sample an average can be calculated and thus improve measurement. The later achievable accuracy from the whole system is not really known. According to the voltage step of $1mV$ a resolution of 2500 values is needed. This is $2^{11.3}$ bits, which means 12 bits plus one bit for noise gives 13 bits of needed resolution at least. Because of the slow measurement $\Sigma\Delta$-converters can be used to get maximum accuracy. An interesting chip is the CS5530 from Cirrus Logic. Among numerous parameters in the choice of an ADC the most important for the CS5530 were:

- linearity error of 0.0015%
- several configurations for power supply, separation of analog and digital
- bipolar input
- up to 3840 samples per second at 13 bits, 120sps at 17 bits
- 50Hz rejection
- gain/offset
- SPI interface

To set up operation the ADC has to be initiated with a sequence and programmed. The IC includes three 32bit registers to be set for measurement[2]: the configuration register and the gain- and offset register. For initial operation the gain should be 1 and the offset zero. The configuration register is written with all zeros except for:

- Bit 11: 50sps (moderate speed and maximum power-net frequency suppression)
- Bit 19: a factor of $\frac{5}{6}$ to support European power-net frequency
- Bit 25: sets the voltage reference to $2.5V$

The HEX code for this registers:

ConfigReg $0x02080800$

GainReg $0x01000000$

OffsetReg $0x00000000$

More details in programming have to be developed when the whole system is running. The values for these registers could be seen as a fail safe or initial configuration.

3.2.2 Suppressor electrode

The suppressor electrode will need to have an adjustable voltage from $0V$ to $-150V$ with almost no current drawn. It should also have a low ripple voltage. A part that was easy to integrate was found from the company Ultravolt, with the US-series DC-DC Converters. These small pcb-mounted DC/DC converters offer a linear adjustment from $0V$ to $-200V$ of the output and a monitoring output in one case. It works with $11.5-15.5V$ and a ripple of $5mV$ for low currents.

3.3 Controller & Interfaces

Because of experiences at IRF with ARM-processors it was suggested to use the development board LPC-P2148 from Olimex as the micro controller. This inexpensive board is used for an interface description. For documentation see the document on the pages from NXP and the corresponding ARM-processor[2]. The controller is the head of the whole BCMS project and represents the interface to a moving table (1 axis), a scanner (2 axis), a sensor head and the present server in the calibration lab which collects the data and offers the human interface. In the end the aim is to send a command and receive a profile, so no calculation time on other computers is needed. The controller interfaces to the following devices:

3.3.1 Motor controller

The intended communication should use the serial port (RS232). This communication is internal and thus it is not really a constraint. Both boards have more possibilities like SPI or USB. The board's intelligence should be used to minimize communication. But in a simple way for each pixel one command is sent which gives no more than 10 commands a second. It is recommended to see the documentation for the desired model TMCM-351-E-TMCL[3].

[2] `http://www.nxp.com/acrobat/datasheets/LPC2141_42_44_46_48_4.pdf`

[3] `http://www.trinamic.com/tmc/media/Downloads/modules/TMCM-351/TMCM-351_manual.pdf`

3.3.2 Power supply

It is not intended to record any housekeeping values except for the high voltage parts. Both monitoring outputs should be stored and displayed to the user. The onboard 10 bit ADC is sufficient for this. The values have to be stored together with each profile.

The suppressor electrode gives out $0 - 2.5V$.

$$V_{SE} = V_{monSE} \cdot 80$$

The CEM board gives $0 - 3V$.

$$V_{CEM} = V_{monCEM} \cdot 1666$$

To show them to the user, the values have to be displayed via panels. It could be done by an SPI-controlled LED panel and using the measured values from the controllers ADC or by panel voltmeters and appropriate resistor dividers. In this case it might be useful to connect the meters directly to the outputs to avoid a chain of voltage-factors.

3.3.3 Sensors

The Faraday cup measurement will be accessible via the ADC's SPI bus (converted current). The SPI is also needed to set up the operation of the ADC. For each pixel one value should be stored together with the position.

The signal from the CEM is to be counted within a well-defined period. Two counter inputs will be needed. One is creating a window suitable to the system speed (at least $100ms$ are needed) and the other counter detects the pulses. Two different profiles are to be scanned: a fast one and a full one. The fast profile is a cross with 23 values and the full one is a raster with 144 values. Each value consists of at least three data parts: the position (8 bit), the voltage of the Faraday cup (24 bit) and the counts of the CEM (20 bit).

A total full profile would then have a size of $144 \cdot 52bit = 7488bit \approx 1kbyte$. To every profile have to be added: the voltages from the CEM, the suppressor electrode and the grid current as well as a time stamp. It could be necessary to include the grid value to every pixel, for determining the stability of the beam and eventually declare the measurement as faulty if it is too instable or use the grid values in order to normalize the sensor values. This has to be done on the server because the measurement of the grid is connected to it. Using time stamps on each system will ensure correlation of all values.

3.3.4 Server

The connection to the server is established via a serial port with a data rate of $56kbps$.

3.4 Power considerations

To start designing a power supply one has to know all the necessary voltages and currents. The system consists of the following parts:

Part	Voltage	current
Motor & Controller	$12V$	2.5A (peak)
OpAmp	$\pm 2.5V$	1.3mA
ADC analog	$\pm 2.5V$	8mA
ADC digital	$3.3V$	1mA
A101	$5V$	10mA
micro controller	$5V$	100mA
Suppressor Voltage	$12V$	50mA
CEM High Voltage	$12V$	100mA
CEM HV	$\pm 5V$	50mA

Table 3: Voltages and Currents

All currents are taken from the data sheets except the CEM's which are based on previous experience. The digital section of the ADC will be powered from the controller board to avoid voltage level problems on the SPI-bus. The HV board from the CEM is designed to run on $15V$ but due to some margin it is possible to run it with $12V$ too. All smaller voltages can be drawn from $12V$ with the following chain:

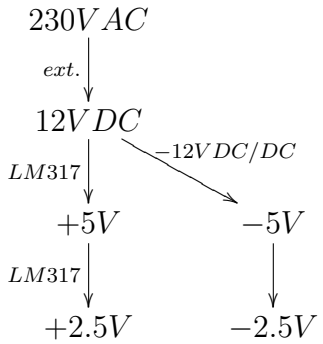

The first stage is to get a DC voltage. An external supply offers here the advantage to have the $50Hz$ as far away as possible. They are also very

common and cheap. To ensure enough power for the motors especially when running on a relative low voltage a minimum current of $3A$ is needed. The negative voltage is generated by a small DC/DC converter. Here not much power is needed. From the table one can get the current usage in summing up the halves of the related currents: $0.7 + 4 + 25 \approx 30mA$. A choice was made with the TMR1212 from Traco Power.
The next stage is the $\pm 5V$ conversion. The use of linear voltage regulators (LVR) will give a good and stable voltage. The LM317 have $40dB$ of ripple rejection until $100kHz$, they are very common and versatile parts. The negative pendant is the LM337. The positive $5V$ needs a closer look at the power consumption because most parts are connected to it including the third stage with $2.5V$. First the power dissipation P_5 has to be calculated from the currents.

$$I_5 = 0.7 + 4 + 1 + 10 + 100 + 25 = 141.7 \approx 150mA$$

$$P_5 = 150mA \cdot (12V - 5V) = 1.05W$$

From the data sheet the thermal resistance from the TO-220 housing to the junction is given with $50\frac{K}{W}$. So the temperature drop is:

$$\Delta T_5 = 1.05W \cdot 50\frac{K}{W} = 52.5K$$

The maximum junction temperature is $125°C$ which gives enough margin. Anyway a small heatsink will be installed which lowers the drop to $27K$ and gives a maximum allowable current of $\approx 570mA$.

The third stage of voltage regulators will feed the current to the voltage converter and the analog section of the ADC. The same LDR's will further increase noise immunity especially when placed close to these parts.

3.5 Schematic & Layout

Two PCB were made in order to operate the sensor: the Front-end electronics (FEE, see appendix C) and the power board (see appendix B).

The FEE should be the support for the evaluation board from the LMP7721 and contain the ADC as well as the A101 part. Also the 2.5V stage will be on that board to ensure most stable voltages. The relay will be glued on the evaluation board with its pins upside-down into the air.

The powerboard is equipped with the DCDC converters for the negative low voltages and for the suppressor electrode ($-12VDC$ and $-200VDC$), the LVR's for 5V, and connectors for control and power.

Only 2-sided boards can be manufactured directly at IRF with a common process. Hereby copper plates with covered photoresist are exposed to light and then etched away in a chemical process.

Both sides are etched in such a way that the traces are formed by etching away two borders. So large areas of copper will remain on the boards which are assigned as ground planes.

4 Tests and Results

To test the sensorhead and the related electronics an experimental setup was built. The main issue is to show that the sensor is working and that the signal transmission as well as the front end electronics are working. It should also show the overlap of equivalent beam currents between the Faraday cup and the Channel Electron Multiplier.

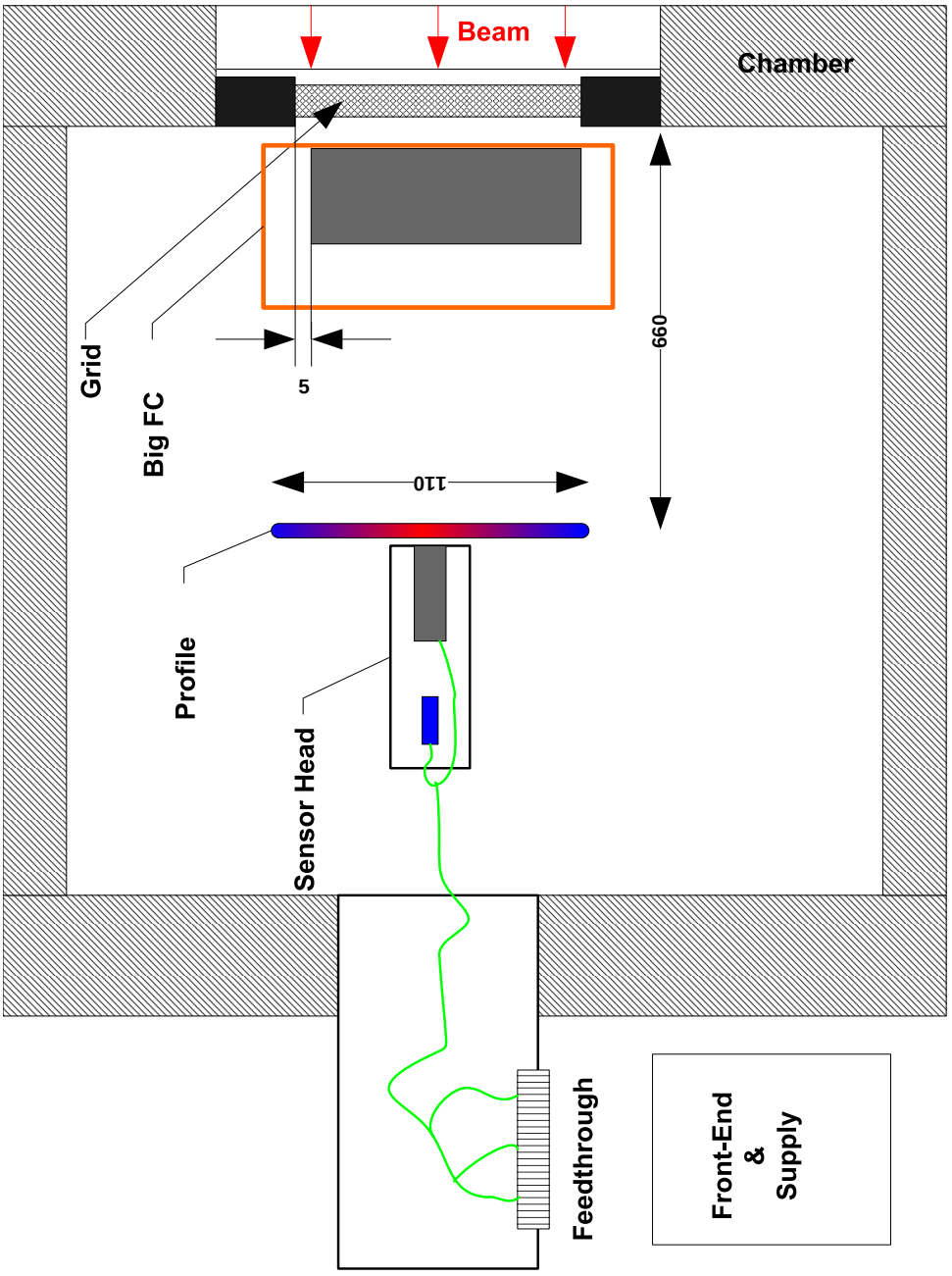

Figure 15: Setup of experiment

4.1 Setup

4.1.1 Beam

The beam is created out of positive Nitrogen ions with a total current of $50pA$. It was assumed that with a total beam current from $10pA$ to $100pA$ the overlapping dynamic range between the Faraday cup and the CEM is shown. A normal beam diameter of $50mm$ should give $2-5pA$ maximum in the Faraday cup and therefore definitely reach the maximum count rate of the CEM.

4.1.2 Mechanical

The present 4-axis table is used to move the sensor head through the beam. The sensor head was placed electrically isolated on a small block. The block was needed to achieve the correct height due to restrictions from the table, so that the sensor could be moved completely through the beam. The initial position was chosen to be approximately in the middle of the beam.

axis	initial	absolute
x	0	13
y	0	-5.5
w	0	38
z	0	-59

Table 4: Table positions

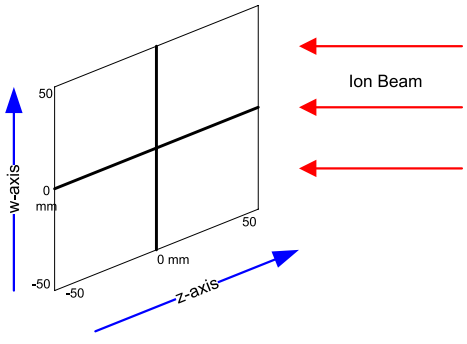

Figure 16: The scan pofile

4.1.3 Electrical

For testing equipment the chamber provides a plate with several connectors of different types: Cannon, SMA and LEMO. The higher voltages were feed through LEMO whereas the rest is done with SMA. Of great importance is the grounding and shielding. The sensor head features a single ground wire which is connected to its housing. The isolation from the table prevents current loops. All shields and grounds are connected to the plate at the chamber in a star-like way. Between this plate and the pigtail of the sensor some leftover test cables were used from other experiments. The Front-End Board was put in a closed metal case which was also grounded to the plate from the chamber.

4.1.4 Measurements

The data is collected manually with the following equipment:

Value	Device
FC voltage	HP34401A
CEM counts	HP5301A
Grid current	Keithley 616
big FC	Keithley 610C

Table 5: Devices for Measurement

Because of manual scanning and manual recording of the measured values, a long time is needed to get one profile. The whole profile took around one hour to complete which is significantly longer than the scanner will need ($\approx 5min$). For each point the grid current at the beam entrance is recorded to normalize the values later. This is important because of the beam instability and the long time needed to get a full profile.

With the current of $\approx 50pA$ one should get pixels with currents high enough to saturate the CEM but also low enough to get valid values from both sensors at the same point. The sensor was moved in steps of $10mm$ to get a profile with 121 pixels which is an area of $110 \times 110mm$.

To begin measurements the Suppressor Electrode voltage and the CEM operational point have to be determined. The CEM has to be characterized before each measurement to know what the condition it is in, especially when using older ones. The suppressor voltage only has to be determined once. It may be adjusted when using higher energetic particles or currents.

In figure 17 one can see that the SE voltage had hardly any influence on the reading, which tells us that not many electrons are escaping and

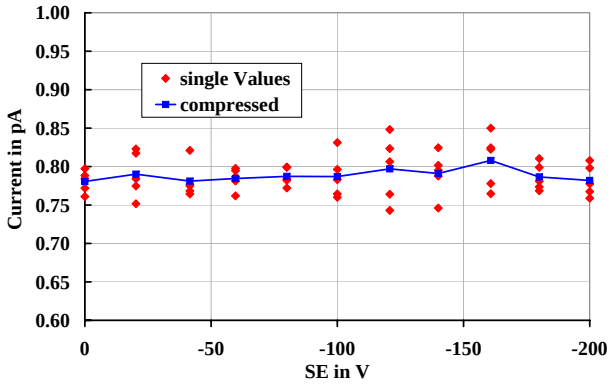

Figure 17: Output over SE voltage

no significant leakage arises from the voltage. It may be that with higher currents one can see some electrons escaping. In the measurements $80V$ were used which is a monitor voltage of $1V$.

The CEM operational point is moving with the total accumulated counts over the lifetime of the CEM.

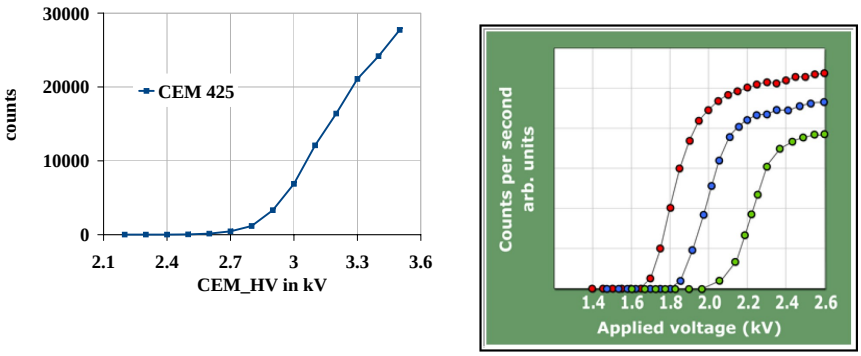

Figure 18: Counts over CEM voltage

In Figure 18 one can see the left diagram taken with the CEM used in this thesis and to the right a data plot from Dr.Sjuts with the red curve as a new CEM and the green as the oldest CEM. The test shows that the CEM used for initial tests is very old and even misses the operating plateau. The data expected is therefore only of relative quality. To use it anyway a voltage

of $3.3kV$ was applied. Before final installation of the system the old CEM will be replaced by a new one.

4.2 Results

To obtain a profile from the Faraday cup representing the real beam, the data was pre-processed. Each reading was normalized with the grid current to cancel out intensity instabilities, an offset was subtracted and the value was geometrically corrected (c_{geo1}). The offset (V_{offset}) was determined by using measurements out of the beam and calculating the average. The geometric factor is due to the circular opening of the Faraday cup and the movement in steps of its diameter plus the hole for the CEM. The factor scales the measured current up to the area of a square with the diameter as edge length and gives a value of:

$$c_{geo1} = \frac{\pi}{4}(1 - \frac{d_{CEM}^2}{d_{FC}^2}) = 0.754$$

So the current in each pixel is determined by the following equation:

$$I_{pixel} = -\frac{\frac{I_{grid-norm}}{I_{grid-measured}} \cdot V_{measured} - V_{offset}}{R_f \cdot c_{geo1}} \tag{7}$$

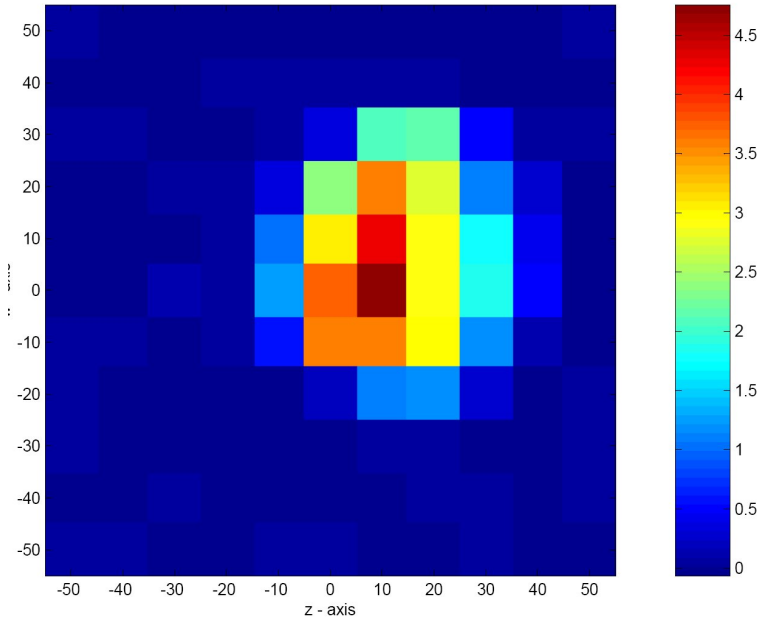

Figure 19: Profile taken from FC - values on axes are in mm and in the legend in pA

The profile shows a typical shape. To show that the profile is reasonable the summation of all values should give the total current of the beam. The measurements gave $59pA$ which is in range with the measured total current of $51pA$.

The CEM profile is made out of counts which are also normalized with the grid current. There was also relative high dark-count rate in the system which is subtracted with an offset. The profile should give a comparable figure.

$$n_{pixel} = \frac{I_{grid-norm}}{I_{grid-measured}} \cdot n_{measurement} - n_{offset} \tag{8}$$

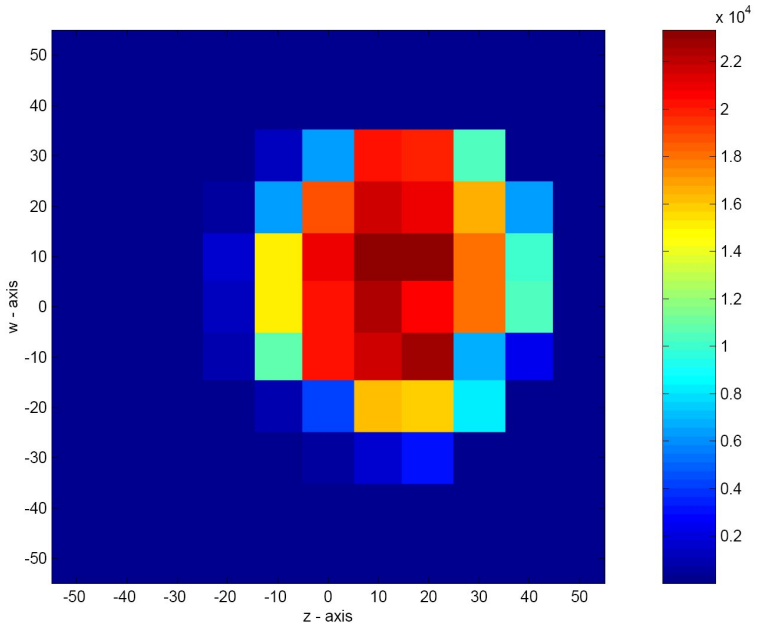

Figure 20: Profile taken from CEM - values on axes are in mm and in the legend in counts per second

The profile shows the same distribution as the FC before. It is slightly bigger and not as pointed as the FC profile. To show the direct intercept the counts from the old CEM have to be fitted to the current values of the Faraday cup. This is usually done just by multiplying the counts with the elementary charge and geometric fit. In this system a current of $1pA$ should give a count rate of $\approx 250kHz$. A CEM tends to saturate or paralyze on higher count rates. The fast solution to this and to get a first value is just to take values from both curves where either the CEM is not saturated and the FC is already out of its noise level. One point meeting these requirements is $[z, w] = (10, -20)$.

$$c[pA^{-1}] = \frac{n}{I} = \frac{15989}{0.813} \approx 20000\frac{1}{pA} \tag{9}$$

More exact is real fitting or modeling with a behavior of the CEM-FEE-Combination as either non-paralyzable or paralyzable according to Wuest[7]. Paralyzing is the effect that occurs when the CEM's count rate is decreasing even if the current is rising. Hereby it is hit with so many charges that the channel inside is not able to serve the full amount of charges necessary to create pulses that are detectable. Because the data does not show this effect the system in this state can be assumed to be non-paralyzable which simplifies the mathematics. Otherwise numerical solutions would be needed. The formula describing the behavior is:

$$\mu = \frac{\nu}{1 + \nu\tau} \cdot c_{eff} \tag{10}$$

where μ is the count rate that the CEM shows, ν is the true count rate derived from the current measured by the FC, τ is the time constant of the whole system including discriminator and c_{eff} as an efficiency factor due to the degradation of the CEM. In a diagram with CEM current over FC current a fit can be done. A value for c_{eff} can be obtained from equation 9 where I is converted into a count rate:

$$c_{eff} = \frac{n}{I} = \frac{n \cdot e}{I \cdot c_{geo2}} = \frac{15989 \cdot e}{0.813pA \cdot 0.04} \approx 0.1 \tag{11}$$

The time constant τ is at minimum the pulse length from the discriminator A101 with $250ns$. For the data shown τ was determined with $6\mu s$ and c_{eff} with 0.16 as shown in figure 21.

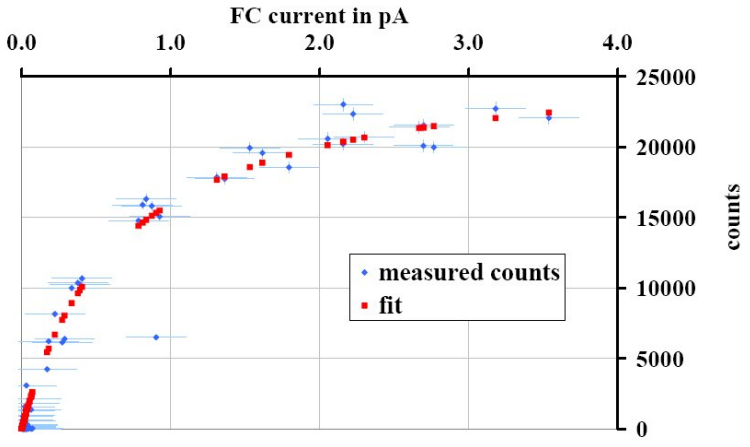

Figure 21: Fitted curve from CEM as a non-paralyzing system

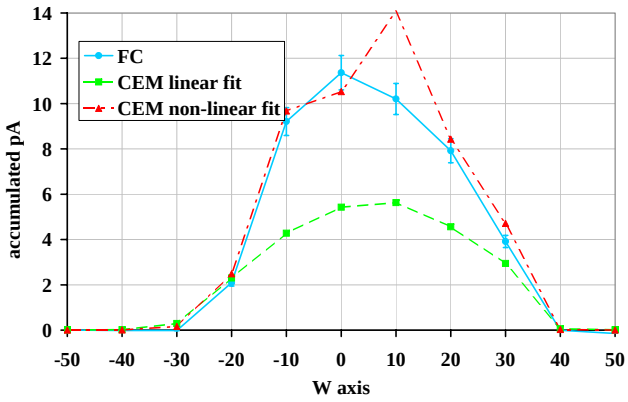

Figure 22: Collapsed z-axis

In figure 22 the z-axis was collapsed. The green curve is the linear fit and the red one is the modeling (non-linear). Figure 23 shows that the CEM starts to saturate at around $1pA$. In the diagram of figure 24 the CEM principle shows clearly its benefits by having a resolution below $1fA$ when the FC signal is just noise.

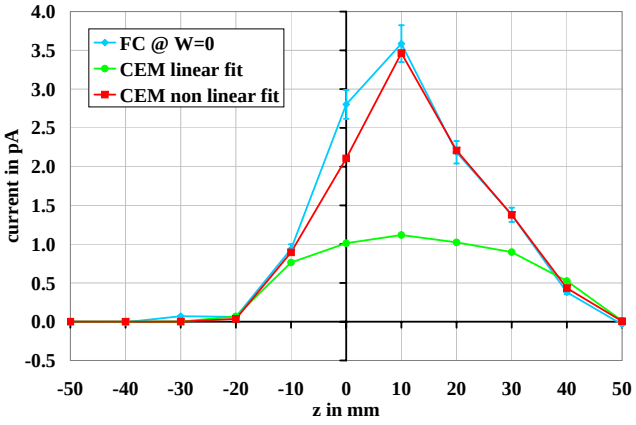

Figure 23: A cross-section at w=0 to show signals at higher currents

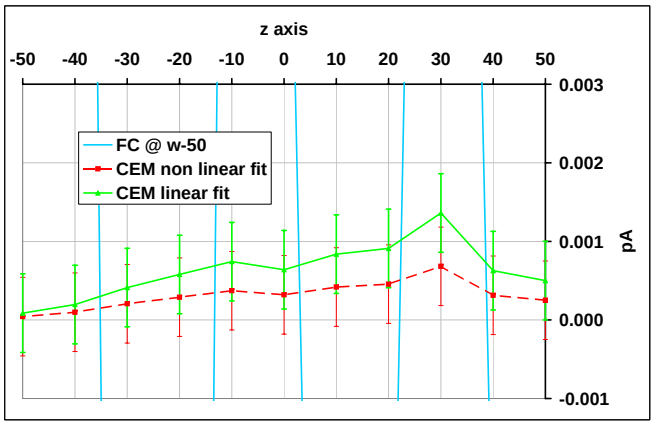

Figure 24: A cross-section at w=-50 to show signals at lower currents

4.3 Discussion

The data shows good performance and that the electronic equipment is working. The total summation with $59pA$ shows a tendency of more current than the total measurement with the big FC. However, measurement with the big Faraday cup has at least an error of 10%. From experience with the measurement an expected total uncertainty of the current in the Faraday cup is $100fA + 5\%$. The summation of all 121 values gives a total uncertainty of $\approx 13pA$. So the measurement is in range but indicates probably systematic errors.

The real current from the small Faraday cup passes three stages: the cup itself and transmission, the voltage conversion and the voltage reading. In each it gains uncertainties of random and systematic kinds. The uncertainties are shown in table 6 with their approximate values.

Error	Value	Kind
ion source	measured with grid	random
leakage	$\approx 10 - 100fA$	systematic
noise EM-fields	?	random
noise Johnson	$\approx 1fA$	random
noise piezoelectric	->0	random
Resistor value	1%	systematic
Reading	$0.005\% + 35\mu V$	random

Table 6: Uncertainties in Measurement

The random uncertainties will not cause an offset in all values. The grid current was used to normalize the measured value due to instabilities in the beam. Between the measurements some seconds passed which lowers accuracy as well as a 2% uncertainty of the reading itself. EM-fields and Johnson noise are low disturbances and should not cause the big difference. Also the long measurement time with the HP multimeter of 100 power-net cycles (2s) minimizes them. The reading itself is also not causing much uncertainty. The piezoelectric noise was minimized with a relatively long time until the sensor head came to rest. Within the series $-40mm$ and $-50mm$ on the w-axis 22 values for a zero reading are taken. They showed an offset of $+0.2V$ as average and a standard deviation of $\sigma \approx 0.20V$. This is a high variance and thus an uncertain value but not a constant one. A permanent leakage from higher voltages would cause a more constant and negative offset. The offset of $0.2V$ represents a current of $20fA$.This offset is a current which is leaking out of the system and thus lowers the total

measurement. One can say that this is the total constant leaking of additive and subtractive currents. But it does not explain the too big current in total.

The suppressor electrode does not have significant influence on the current in terms of leaking electrons because that would lower the current. The electron escape is also low because of the long aspect ratio but the electrode could form a lens which collects additional ions. Tests such as comparing the FC with the CEM or higher currents can reveal this effect and show a useful adjustment of the suppressor electrode voltage. Another explanation could be the misalignment of the system grid and the big FC which is questionable. A closer look showed an approximately $5mm$ misalignment between big FC and grid (see fig. 15). It could be possible that the beam is not fully directed into the big FC and is thus losing some % of current.
To fully determine the absolute current further tests are necessary. One would be to use a smaller aperture or try to examine more clearly the leakage or just to have more data to gain better statistical certainty. Normally it is not intended to have the CEM running beside the FC because the high voltage at the anode will likely cause leakage of electrons out of the FC current. But the data in the profile do not show this so far. That it is possible to use both detectors in parallel at all is a huge advantage.

A main issue was to extend the measurement range from the FC downwards with a CEM. Thus the overlapping region is an important point. It is crucial that the CEM is not paralyzed until the FC can give reasonable values. As the figure 23 shows paralyzing is not present up to $3.5pA$ current in the FC, although it seems that this is close to the maximum of its capability. However that proves the overlapping region in equivalent current is large enough to provide a gradual changeover from CEM to FC. The lower the efficiency of the CEM the lower the resolution will be. The best performance will be achieved when the CEM values are fitted in a way that the lowest trusted FC value is just reached. That ensures maximum resolution of the CEM based measurement. In the present system resolutions down to $1fA$ are possible (fig. 24). A new CEM or even some adjustments of the old CEM would allow an easy-to-achieve step into the atto-ampere region where truly single particles are detected.

4.4 Outlook

The whole system has to be placed in a single enclosure. To tune the suppressor and the high voltage of the CEM it would be beneficial to have these values displayed directly at the front-panel. Some fine tuning in the electronics should be done to increase noise immunity. Also some programming has to be done to set up the ADC of the Faraday cup and to run the controller and its connections. The CEM has to be replaced with a new one for full resolution down to single particles. More tests are also needed to further calibrate the measurements (leakage, absolute values). Some of this work such as the new CEM may have to be postponed until the mechanical structure of the scanner is manufactured.

The sensor head gives IRF the possibility to see the intensity profile from their ion beam facility. Even without having the real scanner operating the beam data is already helpful. When the whole Ion Beam Characterization and Manipulation System is operating, new generations of instruments can be characterized faster and more accurate as they are already today.

5 References

References

[1] INC. BURLE INDUSTRIES. Photomultiplier handbook, 1980. http://psec.uchicago.edu/links/Photomultiplier_Handbook.pdf.

[2] Inc. Cirrus Logic. 24-bit adc with ultra-low-noise amplifier, 2009. http://www.cirrus.com/en/pubs/proDatasheet/CS5530_F2.pdf.

[3] National Semiconductor Corporation. 3 femtoampere input bias current precision amplifier, 2009. http://www.national.com/pf/LM/LMP7721.html.

[4] Dr. Sjuts Optotechnik GmbH. Principles of operation, 2009. http://sjuts.com/Introduction_Principles.html.

[5] Jérôme Lescoup. *Mechanical Design for IRF Calibration Facility.* 2009. Internship report – semester 6 at IRF-Kiruna.

[6] John S. Lewis. *Physics and Chemistry of the Solar System.* Academic Press, 2nd edition, 1997.

[7] Wuest M., Evans D.S., and von Steiger R. *Calibration of Particle Instruments in Space Physics.* ESA Communications, 1st edition, 2007.

[8] Ralph Morrison. *Grounding and Shielding Techniques in Instrumentation.* John Wiley & Sons, Inc., 3rd edition, 1986.

[9] Inc. Pulse Engineering. Introduction to transformer magnetics / g022.a, 1999. http://www.pulseeng.com/file.php?3103.

[10] John R. Taylor. *An Introduction to Error Analysis.* University Science Books, 2nd edition, 1997.

[11] Joseph L. Wiza. Microchannel Plate Detectors. *Nuclear Instruments and Methods*, 162:587–601, 1979. http://psec.uchicago.edu/Papers/mcpwiza.PDF.

List of Figures

1 Vacuum chamber for calibration 8
2 Beam scanner with Sensor head 10
3 Sensor head; the front housing surface for the Faraday cup is already passivated with iridite (yellowish) 12
4 Cutaway view of a straight, single-channel electron multiplier, showing the cascade of secondary electrons resulting from the initial, primary radiation event, which produces an output charge pulse. (After J. L. Wiza, Microchannel plate detectors, Nucl. Instrum. Meth., 162:587–601, 1979) 13
5 KBL408 14
6 Gain vs. counts from `http://sjuts.com/CEMModels_Standard.html` 14
7 Fully assambled CEM ready to be mount in the sensor head. The entrance to the left still covered, the 2 resistors in the middle and the anode to the right. 15
8 Housing and Faraday cup; the cup is bed in isolation material, to the right is the suppressor electrode; the red wire is connected to the suppressor electrode and the white on is connected to the bottom of the Faraday cup 16
9 The Sensor head 17
10 Connections of the CEM 18
11 Transmission of CEM pulse via BALUN's 20
12 Connections of HV Board 21
13 Transimpedance Amplifier 23
14 Relay control 24
15 Setup of experiment 31
16 The scan pofile 32
17 Output over SE voltage 34
18 Counts over CEM voltage 34
19 Profile taken from FC - values on axes are in mm and in the legend in pA 36
20 Profile taken from CEM - values on axes are in mm and in the legend in counts per second 37
21 Fitted curve from CEM as a non-paralyzing system 38
22 Collapsed z-axis 39
23 A cross-section at w=0 to show signals at higher currents . . . 39
24 A cross-section at w=-50 to show signals at lower currents . . 40

List of Tables

1 Data from CEM KBL series 14
2 LMP7721 22
3 Voltages and Currents 28
4 Table positions 32
5 Devices for Measurement 33
6 Uncertainties in Measurement 41

A Abbreviations

ADC	analog to digital converter
BCMS	Beam calibration and manipulation system
CEM	Channel Electron Multiplier
DUT	device under test
FC	Faraday cup
FWHM	Full width half maximum
HV	high voltage
IBP	ion beam profiling system
IRF	Institutet För Rymdfysik
MCP	Micro Channel Plate
OpAmp	Operational Amplifier
SE	suppressor electrode
SPI	Serial Peripheral Interface Bus

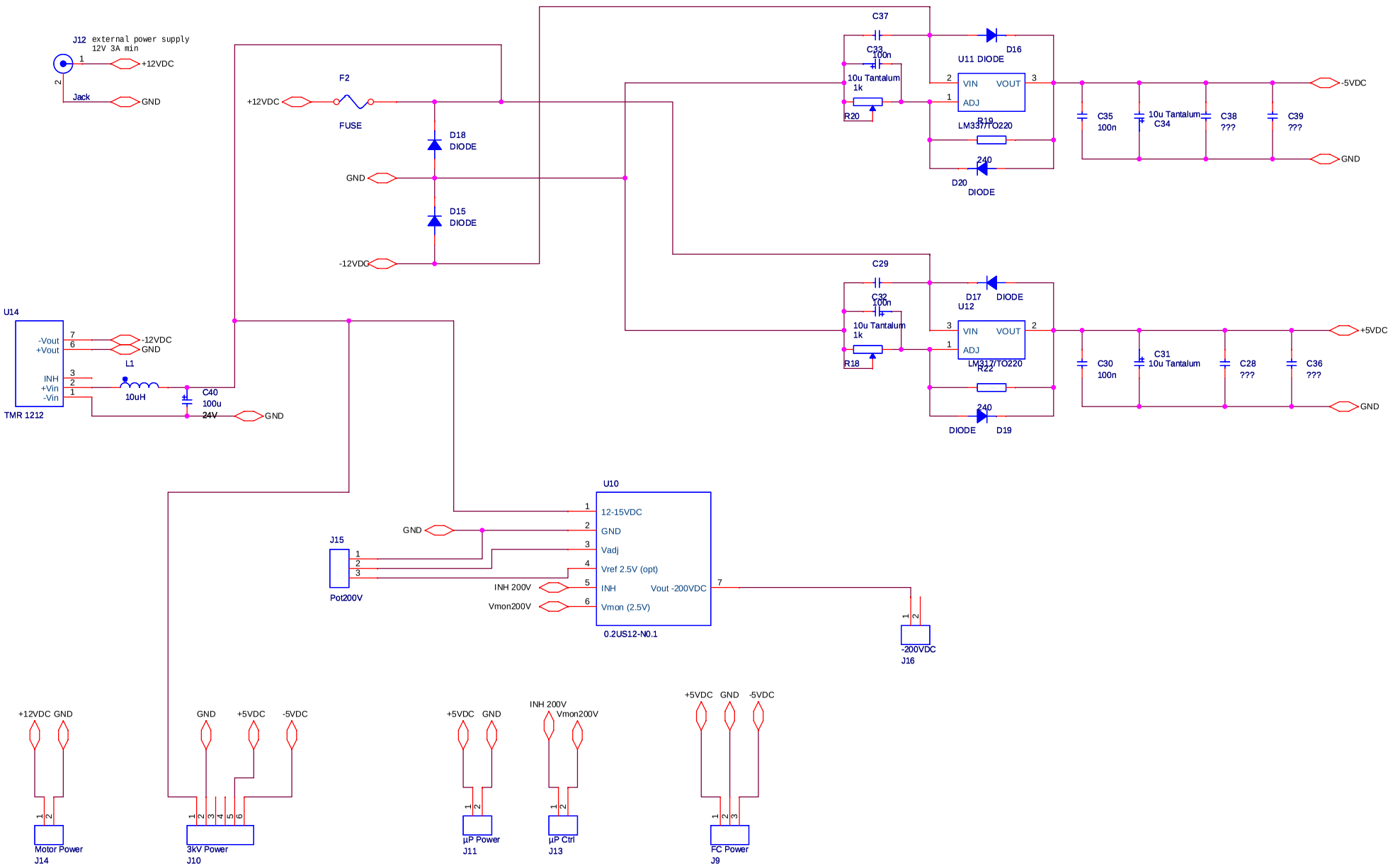

Title	Power Board IBP	
Size A3	Document Number <Doc>	Rev <RevCode>
Date: Wednesday, October 28, 2009	Sheet 1 of 1	

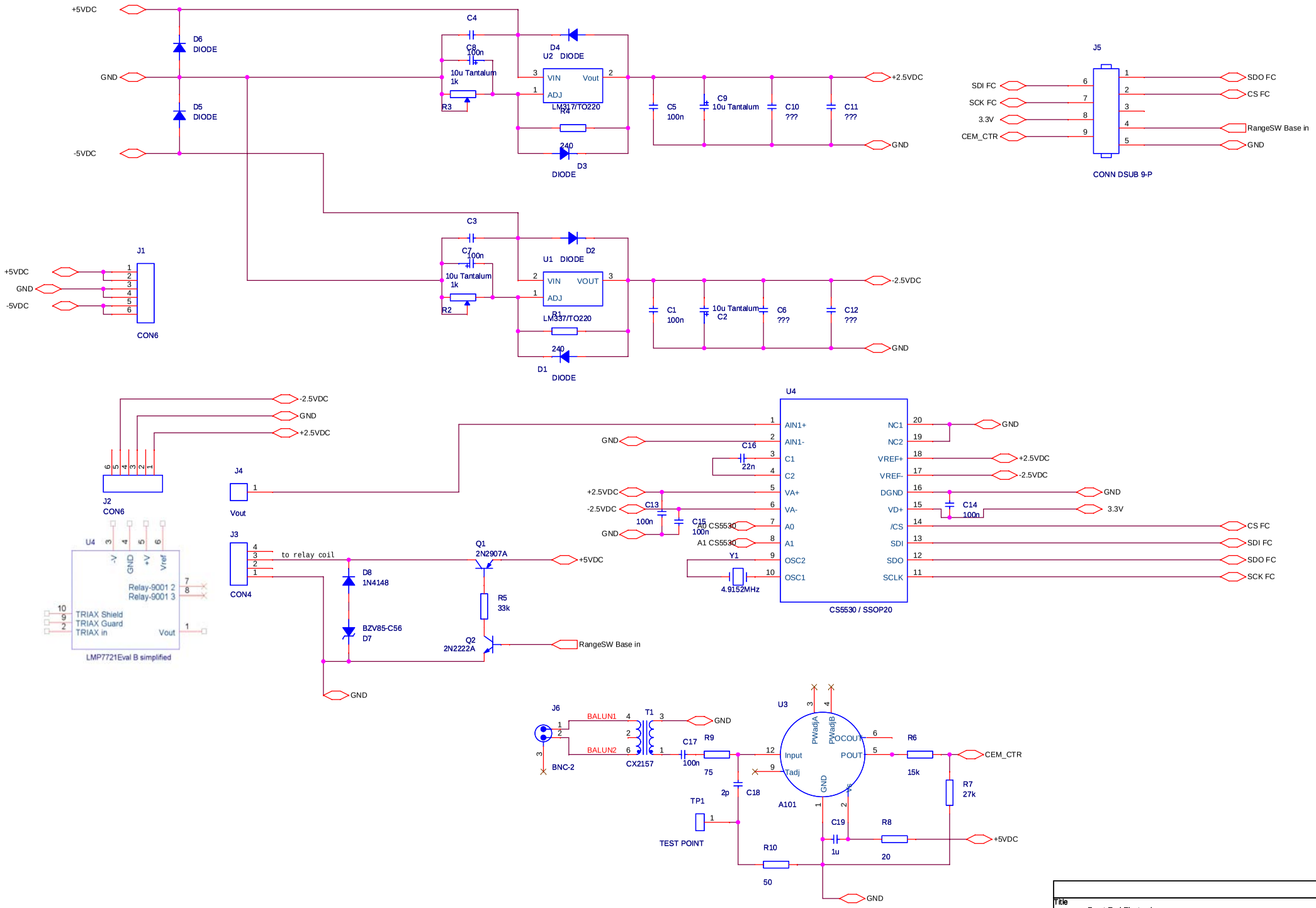

Title	Front-End Electronics		
Size A3	Document Number <Doc>		Rev <RevCode>
Date: Wednesday, October 28, 2009	Sheet 1 of 2		